Developmental Cell
Article

KIF19A Is a Microtubule-Depolymerizing Kinesin for Ciliary Length Control

Shinsuke Niwa,[1] Kazuo Nakajima,[1] Harukata Miki,[1] Yusuke Minato,[1] Doudou Wang,[1] and Nobutaka Hirokawa[1,2,*]
[1]Department of Cell Biology, Graduate School of Medicine, The University of Tokyo, 7-3-1 Hongo, Bunkyo-ku, Tokyo 113-0033, Japan
[2]Center of Excellence in Genome Medicine Research, King Abdulaziz University, Jeddah 21589, Saudi Arabia
*Correspondence: hirokawa@m.u-tokyo.ac.jp
http://dx.doi.org/10.1016/j.devcel.2012.10.016

SUMMARY

Cilia control homeostasis of the mammalian body by generating fluid flow. It has long been assumed that ciliary length-control mechanisms are essential for proper flow generation, because fluid flow generation is a function of ciliary length. However, the molecular mechanisms of ciliary length control in mammals remain elusive. Here, we suggest that KIF19A, a member of the kinesin superfamily, regulates ciliary length by depolymerizing microtubules at the tips of cilia. *Kif19a*$^{-/-}$ mice displayed hydrocephalus and female infertility phenotypes due to abnormally elongated cilia that cannot generate proper fluid flow. KIF19A localized to cilia tips, and recombinant KIF19A controlled the length of microtubules polymerized from axonemes in vitro. KIF19A had ATP-dependent microtubule-depolymerizing activity mainly at the plus end of microtubules. Our results indicated a molecular mechanism of ciliary length regulation in mammals, which plays an important role in the maintenance of the mammalian body.

INTRODUCTION

Mammals have motile cilia on ciliated epithelial cells in various kinds of tissues, such as the brain ventricle, the trachea, and the oviduct. Motile cilia generate fluid flow, which are fundamental to the development and maintenance of the mammalian body (Hirokawa et al., 2006; Ishikawa and Marshall, 2011; Rosenbaum and Witman, 2002; Satir and Christensen, 2007). Defects of ciliary formation and motility lead to fluid flow degeneration and cause human diseases such as hydrocephalus and female infertility (Ibañez-Tallon et al., 2003; Kamiya, 2002; Lyons et al., 2006; Rosenbaum and Witman, 2002). Because ciliary length is an important factor in the control of fluid flow, it has long been assumed that there must be molecular mechanisms that maintain the optimal length of motile cilia (Ishikawa and Marshall, 2011). However, the mechanisms remain largely elusive in mammals. Furthermore, it has not been revealed whether the molecular mechanisms are conserved from protozoa to mammals, although several molecules that control the length of protozoan flagella, a cellular structure homologous to mammalian cilia, have been identified (Berman et al., 2003; Blaineau et al., 2007; Dawson et al., 2007; Tam et al., 2007). The cytoskeleton of motile cilia, called the axoneme, is comprised of two central microtubule singlets, nine outer doublets, and microtubule-associated proteins such as dynein (Ishikawa and Marshall, 2011; Kamiya, 2002; Rosenbaum and Witman, 2002). Kinesin superfamily proteins (KIFs) were originally identified as microtubule-dependent molecular motors that carry out axonal transport (Aizawa et al., 1992; Vale et al., 1985). Mammals have more than 40 KIFs in their genome (Hirokawa et al., 2009; Miki et al., 2001). It has been revealed that KIFs are fundamental to many aspects of biological phenomena, such as intracellular transport of various cargos, microtubule stabilization and depolymerization in neurons, ciliogenesis, and mitosis (Desai et al., 1999; Hirokawa et al., 2009; Homma et al., 2003; Howard and Hyman, 2007; Ishikawa and Marshall, 2011; Kozminski et al., 1995; Rosenbaum and Witman, 2002; Scholey et al., 1985; Zhou et al., 2009). Here, we analyzed the function of a member of kinesin superfamily protein, KIF19A, that localizes to ciliary tips. We present biochemical and genetic evidence that KIF19A has both microtubule-dependent motor and microtubule-depolymerizing activities in vitro and is a key determinant of the optimal length of motile cilia in mice, the deletion of which causes ciliary phenotypes such as hydrocephalus and female infertility.

RESULTS

KIF19A Is a Plus-End-Directed Motor

We have previously identified a partial sequence of KIF19A (Miki et al., 2001). Using the partial sequence as a probe, the open reading frame of KIF19A was identified (Figure 1A). KIF19A is an N-terminal KIF that typically has a plus-end-directed motor activity (Figure 1A). The predicted molecular weight of KIF19A is about 112 kDa. KIF19A belongs to the kinesin-8 family (Gupta et al., 2006; Howard and Hyman, 2007; Lawrence et al., 2004; Mayr et al., 2007; Stout et al., 2011) (Figure 1B). A microtubule gliding assay was performed to test whether KIF19A is a microtubule-dependent motor protein. For this purpose, KIF19A-379, comprising the motor domain and the neck coiled-coil domain, were expressed in *Escherichia coli* and purified by immobilized metal ion affinity chromatography and ion exchange chromatography (Figures 1A and 1C). The purified motor was fixed on anti-penta-His-antibody-coated coverglasses, and tetramethylrhodamine (TMR)-labeled and taxol-stabilized microtubules were flowed in the presence of ATP.

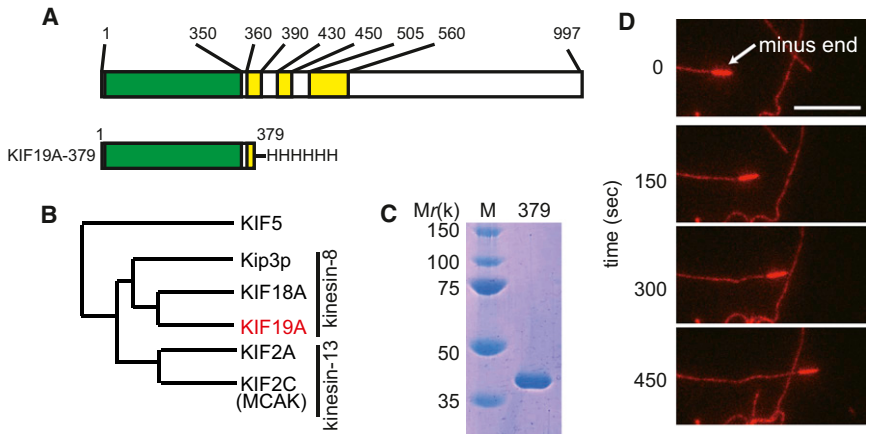

Figure 1. Characterization of KIF19A

(A) Schema showing the structure of KIF19A and a recombinant protein used in this study. Green and yellow regions represent the motor and coiled-coil domains, respectively. Numbers refer to amino acids.

(B) A phylogenetic tree showing that KIF19A is closely related to kinesin-8 members.

(C) KIF19A-379 was expressed in *E. coli* and purified with Co^{2+} beads and SP sepharose beads.

(D) Microtubule gliding assay. KIF19A-379 was fixed on the coverglass, and TMR-labeled and polarity-marked microtubules were introduced into the flow chamber. The minus end was strongly labeled. Scale bar, 10 μm.

See also Movies S1 and S2.

Microtubules were glided on the cover glass (Movie S1 available online). The speed was 21 ± 3 nm/sec (n = 90 microtubules from three independent motor preparations, mean ± SD). The motility assay using polarity-marked microtubules revealed that KIF19A is a plus-end-directed molecular motor (Figure 1D; Movie S2).

kif19a$^{-/-}$ Mice Have Hydrocephalus and Female Infertility

To investigate the in vivo function of KIF19A, we generated KIF19A knockout mice (Figures S1A and S1B). Loss of KIF19A protein expression was confirmed by western blotting on knockout lysates (Figure S1C). While KIF19A was strongly expressed in the oviduct and trachea, these signals were completely diminished in the samples obtained from *Kif19a*$^{-/-}$ mice. Intercrossing between *Kif19a*$^{+/-}$ mice generated *Kif19a*$^{+/+}$, *Kif19a*$^{+/-}$, and *Kif19a*$^{-/-}$ mice with an expected Mendelian ratio, suggesting that the homozygotes exhibit normal embryonic development. However, the *Kif19a*$^{-/-}$ mice showed growth retardation and higher mortality (4 weeks after birth, total 97 mice: *Kif19a*$^{+/+}$, 31; *Kif19a*$^{+/-}$, 57; and *Kif19a*$^{-/-}$, 9). In addition, *Kif19a*$^{-/-}$ female mice were infertile; *Kif19a*$^{-/-}$ female mice paired with wild-type male mice did not become pregnant. To analyze the pathology of *Kif19a*$^{-/-}$ mice, we stained paraffin sections of wild-type and *Kif19a*$^{-/-}$ organs with hematoxylin and eosin (HE). It was revealed that both male and female *Kif19a*$^{-/-}$ mice suffered from hydrocephalus (10 male and 15 female mice) (Figure 2A). Furthermore, the lumens of *Kif19a*$^{-/-}$ oviducts were jammed with mucus and debris, while this was not observed in wild-type oviducts (Figure 2B). The fallopian tube obstruction was always observed in *Kif19a*$^{-/-}$ oviducts that were analyzed by histology (n = 3 in paraffin sections and n = 2 in frozen sections for each genotype). In higher-magnification images, ciliated epithelia were clearly observed in wild-type oviducts (Figure 2C). In contrast, mucus and debris are often observed on the cilia in *Kif19a*$^{-/-}$ sections (Figure 2C). The debris contained nucleus-like structures, suggesting that the debris are dead cells. Thus, these data suggest that the cause of female infertility is fallopian tube obstruction.

Kif19a$^{-/-}$ Mice Had Elongated Cilia

Ciliated epithelial cells are present in the brain ventricle, the oviduct, and the trachea in mammals (Rosenbaum and Witman, 2002; Satir and Christensen, 2007). Cilia generate cerebrospinal fluid flow in the brain ventricle in order to control intracranial pressure. Cilia also help to sweep unnecessary dead cells, debris, mucus, and eggs along the oviduct until they reach the uterus (Ibañez-Tallon et al., 2003; Lyons et al., 2006). Defects of cilia formation and motility often cause hydrocephalus and fallopian tube obstruction in humans and mice (Ibañez-Tallon et al., 2003; Lyons et al., 2006; Rosenbaum and Witman, 2002). Thus, we observed ciliated epithelial cells in the brain ventricle, the trachea, and the oviduct, and found that the ciliary length was longer in all ciliated epithelial cells (Figures 2D–2H). The lengths of brain, tracheal, and oviduct cilia in *Kif19a*$^{-/-}$ mice were 1.8-fold, 1.4-fold, and 2.5-fold longer, respectively, than that in wild-type mice (9.8 ± 0.5 μm in wild-type brain and 17.7 ± 3.1 μm in *Kif19a*$^{-/-}$ brain; 4.6 ± 0.3 μm in wild-type trachea and 6.4 ± 0.6 μm in *Kif19a*$^{-/-}$ trachea, n = 100 cilia from at least two female and two male mice; and 4.9 ± 0.4 μm in wild-type oviduct and 12.5 ± 3.4 μm in *Kif19a*$^{-/-}$ oviduct, n = 100 cilia from five independent female mice, mean ± SD, $p < 0.01$, t test). Furthermore, oviduct cilia were 1.4-fold longer in *Kif19a*$^{+/-}$ oviducts, suggesting that this phenotype is dose dependent (n = 100 cilia from five independent mice; 6.5 ± 0.9 μm in *Kif19a*$^{+/-}$ mice; $p < 0.01$, t test) (Figures 2G and 2H). Oviduct cilia in wild-type samples never exceeded 7 μm, while those in *Kif19a*$^{+/-}$ and *Kif19a*$^{-/-}$ samples were often longer than 7 μm, and we observed several regions (from proximal to distal) in one sample; thus, it is thought that genotypic, but not regional, differences were reflected in these results.

KIF19A Is Localized to the Tips of Cilia

Longer cilia phenotypes suggested that KIF19A might be a ciliary protein. Thus, we first isolated cilia from porcine oviducts and analyzed them by western blotting. Porcine cilia were used because it was difficult to obtain enough ciliary protein from mouse oviducts for biochemistry. Ciliary purification was performed as described (Anderson, 1974) and confirmed by microscopy and a control western blotting using an anti-KIF5 antibody because KIF5 does not enter cilia (Figure 3A) (Dishinger et al., 2010). The anti-KIF19A antibody gave 110-kDa bands in porcine oviducts and porcine cilia. The size was similar to the band obtained on the mouse oviduct sample (Figure 3A). These data suggest that KIF19A is a ciliary protein. To observe the

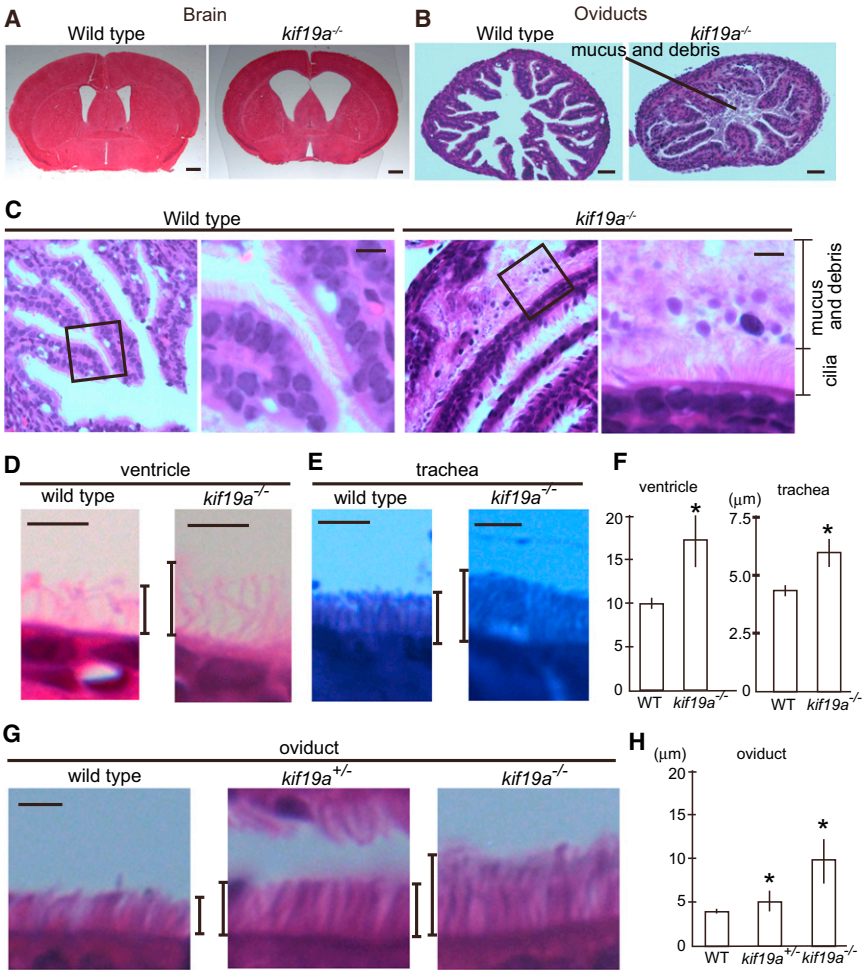

Figure 2. Phenotypes of *kif19*$^{-/-}$ Mice

(A–C) HE staining of wild-type and *kif19a*$^{-/-}$ brain (A) and oviducts (B and C). Brains and oviducts were dissected out from wild-type and *kif19a*$^{-/-}$ mice, fixed by 4% PFA, and subjected to paraffin sectioning and HE staining. (C) *Kif19a*$^{-/-}$ oviducts were jammed with mucus and debris, while wild-type oviducts were not. Representative images are from five independent mice. Scale bars, 500 μm, 100 μm, and 10 μm in (A), (B), and (C), respectively. (D–H) Cilia in brain ventricle, trachea and oviduct. Images in (D) and (E) show HE staining of brain ventricles (D) and toluidine blue staining of trachea (E). Bars, 5 μm. Ciliary length in brain ventricle and trachea was gauged and shown graphically (F). Cilia (n = 100) in (F) were from two pairs of paraffin sections and two pairs of frozen sections. Mean ± SD. *p < 0.01, t test. Images in (G) show HE staining of oviducts in wild-types, heterozygotes, and homozygotes. Scale bar, 5 μm. Ciliary length in oviducts was gauged and is shown graphically (H). Note that ciliary length depends on the amount of KIF19A. Cilia (n = 100) from three pairs of paraffin sections. Mean ± SD. *p < 0.01, t test. See also Figure S1.

localization of KIF19A in cilia, immunofluorescent microscopy was performed. A frozen section of mouse oviducts was stained. Oviduct cilia were observed and it was found that KIF19A is concentrated to tips of cilia (Figure 3B). Furthermore, cilia were isolated from mouse oviducts, fixed, and stained. As a result, one end of isolated cilia gave positive signal (Figure 3C). Coincubation of antigen peptide completely blocked the signal (Figure 3C). Furthermore, tracheal cilia were observed. Similar to oviduct cilia, it was found that tips of cilia gave positive signals (Figure 3D). Staining of *kif19a*$^{-/-}$ sections confirmed the specific staining of the antibody (Figure 3D). Finally, to better observe the localization of KIF19A in cilia in vivo, cultured ependymal cells were observed. It was found that KIF19A is concentrated to the tips of cilia in these cells (Figure 3E). Taken together, KIF19A is a ciliary tip protein.

Longer Cilia Cannot Generate Proper Fluid Flow

To observe the ciliary movement in *Kif19a*$^{-/-}$ mice, time-lapse observations were performed in semidissected living oviducts by differential interference contrast (DIC) microscopy (Shi et al., 2011). Oviducts were dissected out from wild-type and *kif19a*$^{-/-}$ mice, cut into small pieces (about 0.5 mm), and observed under an upright light microscope. We could observe moving cilia under these conditions and again confirmed that the length of cilia was changed in *Kif19a*$^{-/-}$ mice (Figure 4A; Movie S3). The waveform of cilia was analyzed by line tracings of cilia at turnaround points. Abnormal ciliary waveforms were often observed, especially at backward points (Figure 4B). Although the bases of cilia moved, the tips of cilia did not move properly in *Kif19a*$^{-/-}$ longer cilia. Furthermore, while wild-type ciliary tips moved almost simultaneously, *Kif19a*$^{-/-}$ ciliary tips lost the uniformity. In addition, *Kif19a*$^{-/-}$ cilia did not generate proper fluid flow (Figures 4C and 4D; Movie S3). In contrast, wild-type cilia could generate constant fluid flow at or near the surface of ciliated cells (Figures 4C and 4D; Movie S3). These data suggest that the abnormally longer cilia cannot generate proper fluid flow in *Kif19a*$^{-/-}$ mice.

KIF19A Controls the Length of Microtubules Polymerized from Axonemes

Axonemes, which form the cytoskeleton of motile cilia, consist of two central microtubule singlets, nine outer doublets, and microtubule-associated proteins such as outer and inner dyneins (Ishikawa and Marshall, 2011; Kamiya, 2002; Rosenbaum and Witman, 2002). Because the length of cilia was abnormally longer in *kif19a*$^{-/-}$ mice, we tested in vitro whether KIF19A can directly control microtubule polymerization from axonemes. Axonemes isolated from *Chlamydomonas* were mixed with porcine brain tubulin and incubated at 37°C for 30 min (Binder et al., 1975). Various concentrations of the motor domain of KIF19A (KIF19A-379) and 5 mM ATP were added and coincubated with the reaction. In the control experiment, long microtubules were polymerized from the tips of axonemes (Figure 5A). When KIF19A-379 was coincubated, the length of microtubules polymerized from axonemes became shorter depending on the

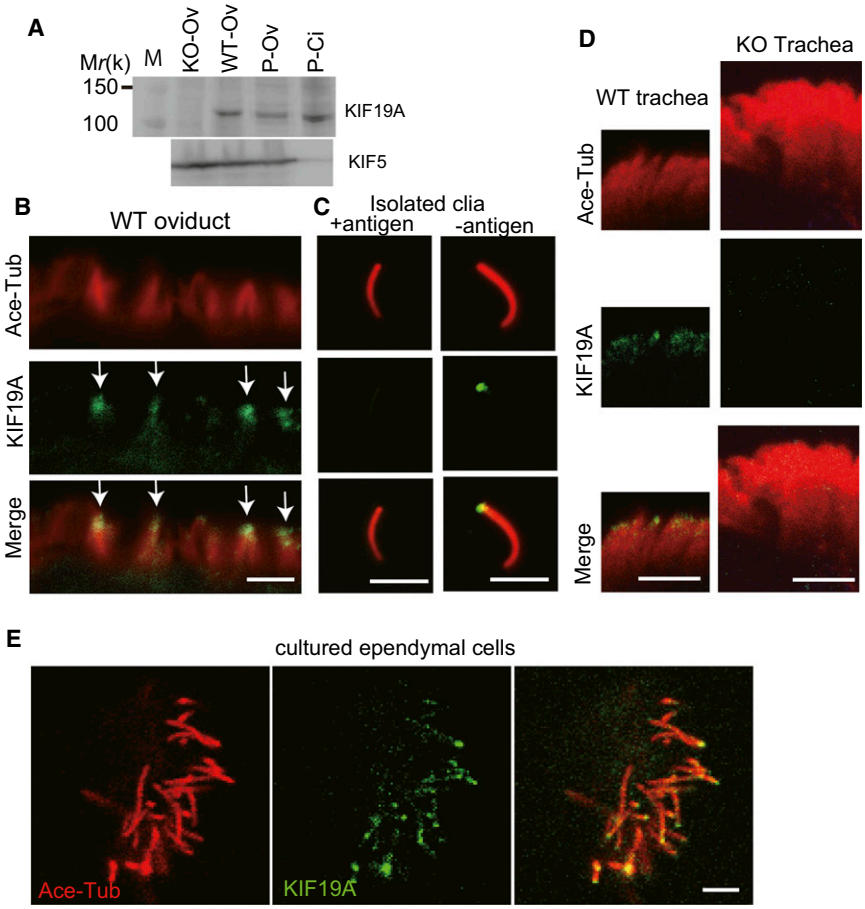

Figure 3. KIF19A Is a Ciliary Tip Protein

(A) Porcine cilia were isolated from porcine oviducts and analyzed by western blotting. Cilia were mechanically released from porcine oviducts. As negative and positive controls, *kif19a*$^{-/-}$ oviducts (KO-Ov) and wild-type oviduct (WT-Ov) samples were electrophoresed together. A 110 kDa band, which is diminished in *kif19*$^{-/-}$ oviducts, was observed in porcine oviducts (P-Ov) and cilia samples (P-Ci). KIF5, a protein that does not enter cilia, is used as a control.

(B–E) Immunofluorescent microscopy using anti-acetylated tubulin (red) and anti-KIF19A (green) antibodies. Mouse oviducts were stained (B), isolated mouse oviduct cilia were stained (C), and antigen peptide was incubated as a control (left panels). Mouse trachea (D) and cultured ependymal cells (E) are also shown. *kif19a*$^{-/-}$ trachea served as a negative control in (D). Scale bars, 5 μm.

concentration of KIF19A-379 (Figures 5A and 5B). KIF19A-379 at 2.5 μM completely blocked microtubule polymerization from axonemes. The concentration dependency is consistent with the in vivo data showing that the ciliary length depends on the dosage of *kif19a* expression (Figures 2G and 2H). These data suggest that the motor domain of KIF19A can directly and negatively regulate the length of microtubules newly polymerized from axonemes. The length of microtubules is a function of microtubule polymerization and depolymerization rates (Mitchison and Kirschner, 1984). Thus, if KIF19A-379 has microtubule depolymerizing activity, the length of microtubules polymerized from axonemes should become shorter. KIF18A and Kip3p, kinesin-8 family members that are closely related to KIF19A (Figure 1B), have both motor activity and microtubule-depolymerizing activity, and they control spindle length in mitotic cells (Gupta et al., 2006; Varga et al., 2006). We hypothesized that KIF19A-379 might have microtubule-depolymerizing activity in order to control the length of ciliary microtubules. To test this, an in vitro microtubule-depolymerizing assay was performed (Desai et al., 1999; Noda et al., 2012). GMPCPP-stabilized microtubules, purified KIF19A-379, and 5 mM ATP were incubated at room temperature for 10 min. As a result, microtubules were depolymerized in a dose-dependent manner (Figure 5C). Adenosine 5′-[β,γ-imide]triphosphoric acid (AMPPNP) is a competitive inhibitor of ATPases and is often used to inhibit the activity of KIFs (Vale et al., 1985). When AMPPNP was added instead of ATP, depolymerization was totally inhibited, even after a 30 min reaction (Figure 5D). Furthermore, KIF19A-379 was found in the microtubule pellet fraction in the presence of AMPPNP (Figure 5D). The AMPPNP-induced binding to microtubules is observed in other KIFs as well (Okada et al., 1995; Vale et al., 1985). These data suggest that the motor domain of KIF19A depolymerizes microtubules in an ATP-dependent manner. To obtain dose-reaction curves, GMPCPP-stabilized microtubules were incubated with various concentrations of KIF19A-379 for 10 min at room temperature, and the ratio of depolymerized tubulin was quantified and plotted (Figure 5E) (Hertzer et al., 2006; Noda et al., 2012). These data were fit to the four-parameter logistic equation (Equation 1) to calculate the half-maximal effective concentration (EC_{50}) of KIF19A-379. The EC_{50} values from three independent motor preparations were 253, 271, and 230 nM, respectively. AMPPNP completely blocked microtubule depolymerization in all three samples (Figure 5E).

KIF19A Depolymerizes Microtubules Mainly from the Plus End

Microtubule depolymerization was observed by time-lapse microscopy. To discriminate the plus and minus ends of microtubules, segment-labeled microtubules were used as substrates (Desai and Mitchison, 1998; Desai et al., 1999). When 25 nM KIF19A-379 was incubated with segment-labeled microtubules, the depolymerization dominantly started from the plus end of microtubules (Figure 6A; Movie S4). The depolymerization speeds were 17.9 ± 3.8 nm/s and 1.0 ± 0.6 nm/s for the plus ends and minus ends, respectively, of GMPCPP-stabilized microtubules (Figure 6C; n = 20 microtubules from three independent motor preparations). In an additional test at a higher concentration of KIF19A-379, 250 nM, KIF19A-379 depolymerized the plus ends and minus ends of microtubules at 106.3 ± 25.4 nm/s and 14.5 ± 3.0 nm/s, respectively (Figure 6C). Thus,

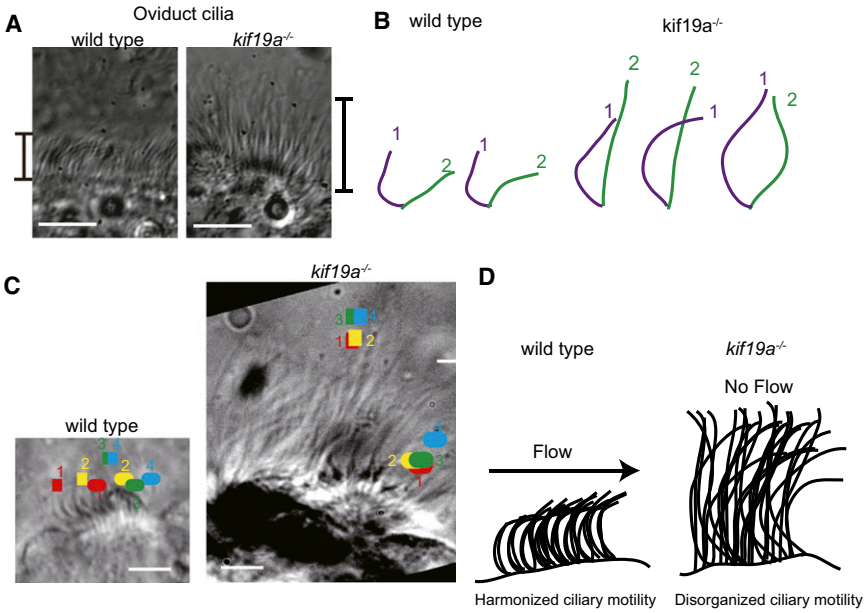

Figure 4. Defects of Fluid Flow

(A) Wild-type and *kif19a*$^{-/-}$ oviducts were dissected, cut into small pieces, and observed under a microscope. Cilia could be observed. Scale bars, 5 μm.

(B) Line tracings of wild-type and *kif19a*$^{-/-}$ cilia at the turnaround points were extracted from Movie S3. Forward (1, purple) and backward (2, green) points are shown. Representative tracings are presented. While wild-type cilia had clear strokes, *kif19a*$^{-/-}$ cilia did not. Tips often did not move properly.

(C) The motility of small dust, which could clarify the fluid flow, was plotted from Movie S3. Wild-type cilia generated constant flow, but *kif19a*$^{-/-}$ cilia did not. Scale bars, 5 μm.

(D) The schema shows the summary of Movie S3.

the depolymerization rate depends on the concentration of KIF19A. AMPPNP completely blocked the depolymerization (Figures 6A and 6C), consistent with the results of sedimentation assays (Figures 5D and 5E). Strong fluorescent labeling of microtubules sometimes changes the property of microtubules (Desai and Mitchison, 1998). To exclude the possibility that the segment labeling changed the property of microtubules, evenly labeled microtubules were depolymerized by KIF19A-379. In this condition, one end of microtubules was dominantly depolymerized, which is similar to the results of segment-labeled microtubules (Figure 6B). The depolymerization rate was similar to those of the plus end of segment-labeled microtubules. Thus, it would be the plus end. These results suggest that the motor domain of KIF19A has plus-end-dominant microtubule-depolymerizing activity.

DISCUSSION

Here, we suggest that KIF19A maintains the optimal length of motile cilia by depolymerizing microtubules at ciliary tips (Figure 7). As the fluid flow generated by motile cilia is essential for the maintenance of the mammalian body and the ciliary length is an important factor in fluid flow, it has long been assumed that ciliary length control mechanisms exist and are fundamental to mammalian health (Ishikawa and Marshall, 2011). We observed the motility of abnormally elongated cilia in *Kif19a*$^{-/-}$ mice and presented firm experimental evidence that elongated cilia cannot generate proper fluid flow as anticipated in theory (Figure 4). *Kif19a*$^{-/-}$ mice suffer from such ailments as hydrocephalus and female infertility, and they tend to die earlier than do wild-type mice. Thus, a molecular mechanism maintaining the optimal length of motile cilia is fundamental to mammalian health. Because it is difficult to perform genetic screening of ciliary length mutants in vertebrates, molecular mechanisms that determine the optimal length of motile cilia have remained largely unidentified in mammals, although a few molecules that limit the length of immotile cilia have been identified (Omori et al., 2010; Tammachote et al., 2009). We suggest that KIF19A is a key determinant of optimal length of motile cilia on mammalian ciliated epithelial cells. Protozoan flagella are homologous to mammalian cilia in cellular structure (Rosenbaum and Witman, 2002). Using molecular genetics, several factors that regulate flagellar length have been identified in unicellular organisms (Berman et al., 2003; Blaineau et al., 2007; Dawson et al., 2007; Tam et al., 2007). Among these factors, Kinesin-13, a class of microtubule-depolymerizing kinesin, has been shown to control flagellar length in *Leishmania* and *Giardia* (Blaineau et al., 2007; Dawson et al., 2007). However, this mechanism is not conserved even within protozoa. In *Trypanosoma* and *Chlamydomonas*, kinesin-13 is not involved in flagellar length control (Chan and Ersfeld, 2010; Piao et al., 2009). Thus, until this study, it has been unclear whether the microtubule regulation machinery is conserved in and also required for ciliary length control in higher organisms. Our results strongly suggest that the molecular mechanism controlling microtubule length is required to determine proper ciliary length in mammals. Interestingly, KIF19A was not a conserved homolog of protozoan kinesin-13. While kinesin-13 depolymerizes microtubules from both plus and minus ends of microtubules (Desai et al., 1999; Gupta et al., 2006; Hunter et al., 2003; Varga et al., 2006), KIF19A depolymerizes microtubules mainly from their plus ends (Figure 6). KIF19A is closely related to kinesin-8 family members that control the spindle length in mitotic cells (Gupta et al., 2006; Mayr et al., 2007; Stout et al., 2011; Varga et al., 2006). The reason this difference between mammals and protozoa has evolved is interesting, considering the structural similarity between mammalian cilia and protozoan flagella. One possibility is that the plus-end-dominant depolymerization by KIF19A was more efficient for ciliary length regulation because the plus ends of axonemal microtubules are directed toward the distal end of cilia (Figure 7). Moreover, it should be noted that kinesin-8, but not kinesin-13, can depolymerize microtubules in a length-dependent manner (Varga et al., 2009) that is suitable for the ciliary length control mechanism.

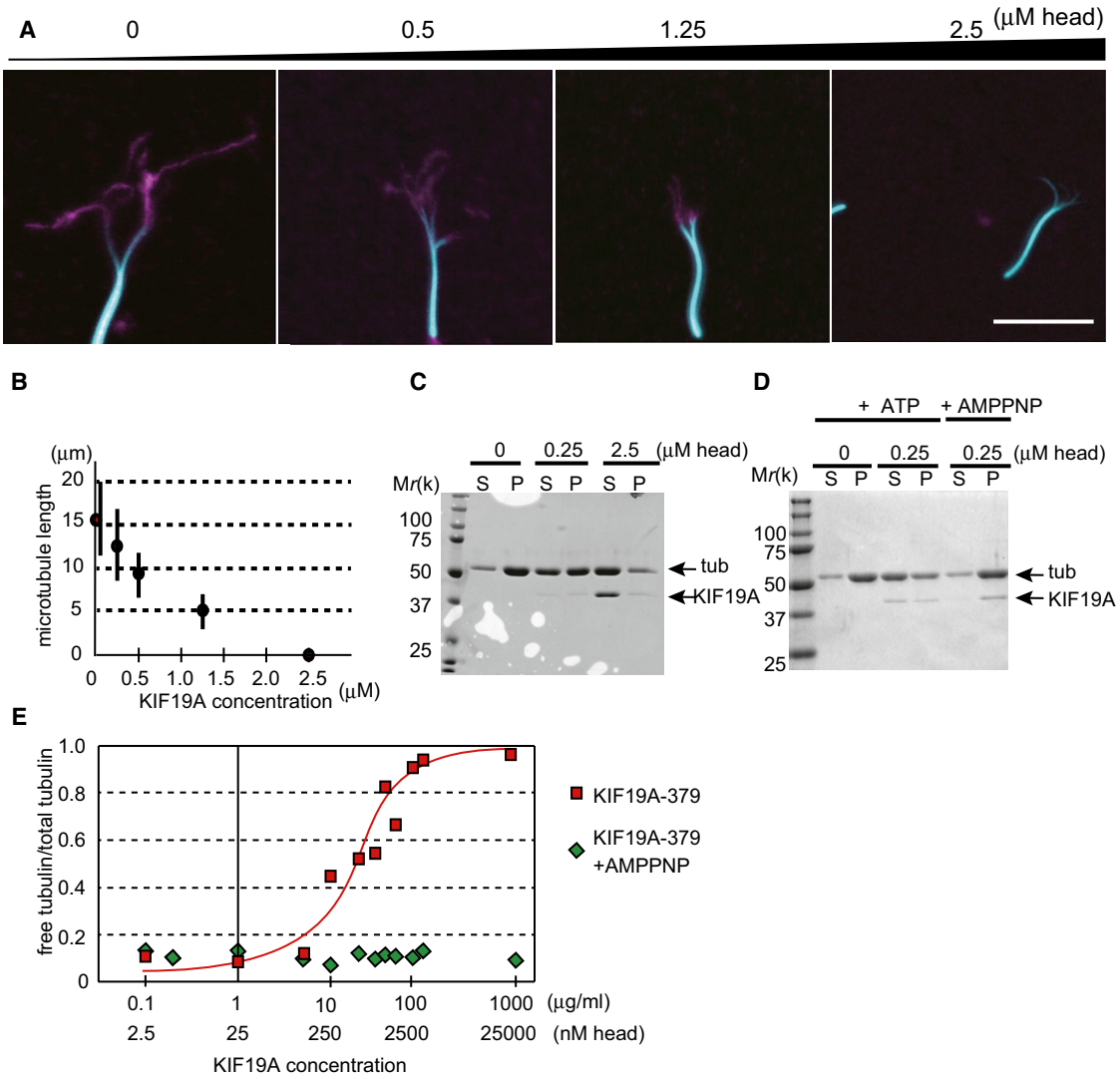

Figure 5. KIF19A Is a Microtubule-Depolymerizing Kinesin

(A and B) Alexa-647-labeled *Chlamydomonas* axonemes (cyan) were mixed with 1.5 mg/ml TMR-labeled tubulin (magenta) in PEM buffer supplemented with 1 mM GTP and 5 mM ATP. Several concentrations of KIF19A-379 were coincubated for 30 min. To avoid confusion, the concentration represents the motor head concentration, although KIF19A-379 forms a dimer. Representative images are shown in (A). The length of polymerized microtubules became shorter in higher KIF19A-379 concentrations. Scale bar, 10 μm. (B) The length of microtubules polymerized from axonemes is plotted. Mean ± SD. Axonemes (n = 20) were from three independent experiments.

(C and D) Tubulin (3 μM) was incubated with 0.5 mM GMPCPP and polymerized at 37°C for 2 hr. GMPCPP-stabilized microtubules were pelleted and resuspended by PEM buffer (final concentration, 10 μM). The indicated concentrations of KIF19A-379 were incubated in the presence of 5 mM ATP for 10 min and centrifuged at 65,000 rpm for 5 min to separate depolymerized tubulin (S) and microtubule (P) fractions (C). Samples were subjected to SDS-PAGE and Coomassie brilliant blue staining. KIF19A-379 (0.25 μM) was incubated in the presence of 5 mM ATP or AMPPNP for 30 min (D) and analyzed as in (C).

(E) Dose-reaction curve made from 10 min reactions. Representative data from three independent motor preparations are shown.

We showed that ciliary length depends on the gene dosage of *Kif19a* (Figures 2G and 2H) and recombinant KIF19A controls the microtubule polymerization from axonemes in a dose-dependent manner (Figure 5). A previous study showed that the gene dosage of yeast *Kip3* is a fundamental factor for the spindle length control mechanism (Su et al., 2011). It is considered that dose dependency is a common character for both spindle length control and ciliary length control.

Interestingly, recombinant KIF19A did not depolymerize purified axonemes per se. It is well established that axonemes, composed not only of microtubules but also of many microtubule-associated proteins, have very stable structures (Ishikawa and Marshall, 2011; Kamiya, 2002; Rosenbaum and Witman, 2002). Furthermore, several studies have suggested that ciliary microtubules are stabilized by posttranslational modifications (Akella et al., 2010; O'Hagan et al., 2011; Wloga et al., 2009). Thus, one possibility is that KIF19A depolymerizes nascent microtubules only, i.e., that it works before ciliary microtubules are stabilized by microtubule-associated proteins and post-translational modifications. Although it does not exclude the first

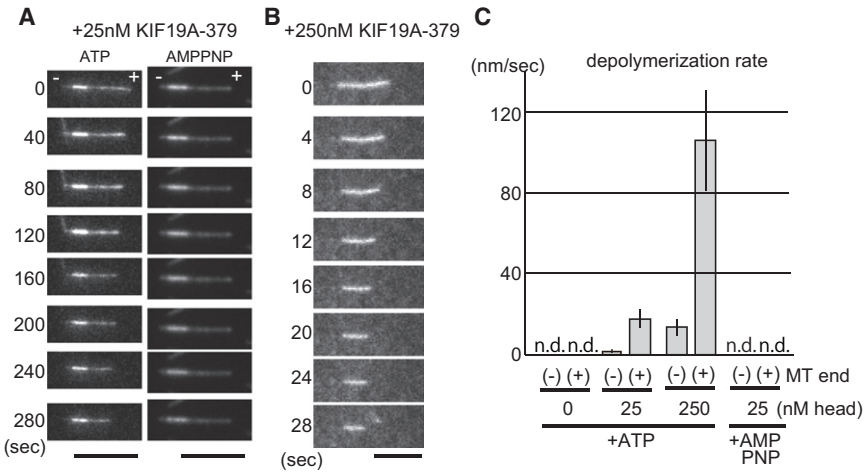

Figure 6. KIF19A Depolymerized Microtubules at the Plus End of Microtubules

(A) Segment-marked microtubules were incubated with 25 nM KIF19A-379 in the presence of 5 mM ATP or AMPPNP. The microtubule was dominantly depolymerized from the plus end in an ATP-dependent manner, although slight minus-end depolymerization was also observed. Scale bars, 10 μm.

(B) Evenly labeled microtubules were depolymerized by 250 nM KIF19A-379. One end of microtubules was dominantly depolymerized. Scale bar, 5 μm.

(C) The depolymerization rate at the plus and minus ends is shown graphically. Note that the depolymerization rate depends on the concentration of KIF19A-379, and that the plus end is dominantly depolymerized. Mean ± SD. n.d.; not detected.

See also Movies S4 and S5.

possibility, another possibility is that additional factors are required to depolymerize mature and stabilized axonemes. Tubulin-modifying enzymes, other microtubule depolymerases, and the ubiqutin-proteasome system are good candidates for cooperative depolymerization of stabilized axonemes (Huang et al., 2009; Hubbert et al., 2002; O'Hagan et al., 2011; Piao et al., 2009; Sharma et al., 2007).

In conclusion, we have identified a molecular mechanism that regulates the length of motile cilia in mice. Identification of factors that regulate or bind to KIF19A would help to elucidate the molecular mechanisms of ciliary length control in mammals.

EXPERIMENTAL PROCEDURES

Full experimental procedures are presented in the Supplemental Experimental Procedures.

Cloning of KIF19A and the Expression of Recombinant Protein

The full-length nucleic acid sequence of KIF19A (NM_001102615.1) was cloned by 5′ and 3′ rapid amplification of cDNA ends. Briefly, a brain cDNA library (Clontech, Mountain View, CA, USA) was used for polymerase chain reaction (PCR) using one primer specific for the motor domain of KIF19A and the other primer for the adaptor ligated at the ends of all cDNA clones. DNA fragments encoding the motor and neck coiled-coil domains of KIF19A (1–379 aa of mouse KIF19A; KIF19A-379) were amplified by PCR, ligated into pET21b vector (Merck, Darmstadt, Germany), and purified as described (Noda et al., 2012).

Antibodies

The COOH-terminal 21-amino-acid peptide, CGPSLPHGSSTFGKDGRLQHN, was synthesized and purchased from Sigma-Genosys (St. Louis, MO, USA) and injected into rabbits. Anti-KIF5 antibody was reported previously (Kanai et al., 2000). Anti-acetylated tubulin was obtained from Sigma. Anti-penta-His antibody was purchased from QIAGEN (Venlo, Netherlands).

Microtubule Gliding Assays

Microtubule gliding assays were performed as previously described (Carter and Cross, 2001), but slightly modified. Fluorescent labeled microtubules and total internal reflection fluorescence microscopy (TIRF) were used instead of unlabelled microtubules and DIC microscopy. For observation, all procedures were performed at room temperature. Time-lapse observation was performed using the ELYRA P.1 system (Carl Zeiss, Jena, Germany) in the TIRF mode.

Generation of *kif19a*$^{-/-}$ Mice

All animal experiments were approved by the Graduate School of Medicine, University of Tokyo, and performed under the University's animal-experimentation rules. The targeting vector was constructed using genomic fragments amplified from the 129/Sv-derived embryonic stem cell (ESC) line CMT1-1 (Chemicon/Millipore, Billerica, MA) with an LA-PCR kit (Takara, Japan), as described (Nakajima et al., 2002). Homologous recombination was confirmed by Southern blot as described (Nakajima et al., 2002).

Histochemistry

Tissues were dissected out from 4-week-old mice, dehydrated through a graded alcohol series, cleared with xylene, and embedded in Paraplast (Oxford Labware, Oxford, United Kingdom). The tissues were serially sectioned (10 μm thick) and stained with HE. Samples were microphotographed using a Leica DM3000 microscope equipped with a DFC290 HD color digital camera (Leica Microsystems, Wetzlar, Germany).

Observation of Ciliated Epithelium

Oviducts were dissociated from wild-type and *kif19a*$^{-/-}$ mice in cold Hank's balanced salt solution. Dissociated oviducts were cut into small pieces (0.1–0.5 mm) and immediately put on a slide glass with medium. Cells were covered by a coverslip (Matsunami, Tokyo, Japan) and observed using an IX-51 upright microscope (Olympus, Tokyo, Japan) equipped with a PlanApo lens (100×, NA 1.35) and CoolSNAP HQ CCD camera (Roper, Trenton, NJ) or Luca (S) EMCCD camera (Andor, Belfast, Northern Ireland).

Microtubule Polymerization from Axonemes

Chlamydomonas axonemes were purified as previously described (Yagi et al., 2009). Microtubule polymerization from axonemes was performed as previously described (Binder et al., 1975), but we used fluorescent labeled axonemes and tubulin. TMR-labeled tubulin and unlabeled tubulin were mixed at 1:10. Alexa-647 axonemes and TMR tubulin (final concentration, 1.5 mg/ml) were diluted in PEM supplemented with 1 mM GTP, 5 mM ATP, and 1 mM dithiothreitol and incubated at 37°C for 30 min in the presence of several concentrations of KIF19A-379. Reactions were stopped by adding an equal amount of PEM supplemented with 2% glutaraldehyde. Axonemes and microtubules were observed with an LSM710 confocal microscope (Carl Zeiss).

Microtubule Depolymerization Assay

Microtubule-depolymerizing assays were performed as previously described (Hertzer et al., 2006; Noda et al., 2012). For quantification analysis, depolymerization assays were performed using GMPCPP-stabilized microtubules. Assays were performed in PEM supplemented with 1 mM dithiothreitol and 5 mM MgATP. The supernatant and resuspended pellet fractions were

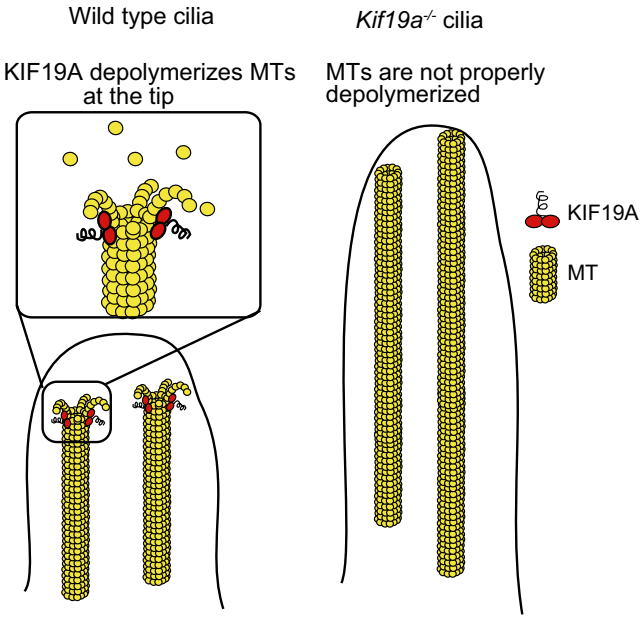

Figure 7. Model
KIF19A is concentrated to the tips of cilia and depolymerizes microtubules in wild-type cilia. In *kif19a*$^{-/-}$ cells, ciliary microtubules are not properly depolymerized, and ciliary length becomes abnormally longer.

analyzed by SDS-PAGE and CBB staining. The data were plotted and fit to the four-parameter logistic equation (Equation 1), and the EC_{50} was calculated using KaleidaGraph 4.0 software (Synergy, Reading, PA, USA), where Response is the amount of tubulin in the supernatant fraction, R_{min} is the baseline, R_{max} is the maximal response, X is the enzyme concentration, and *H* is the Hill slope:

$$\text{Response} = \frac{R_{min} + (R_{max} - R_{min})}{\left[1 + 10^{H*\log(EC50/X)}\right]}. \quad \text{(Equation 1)}$$

For microscopic analysis, the flow-chamber system was used. TMR- and biotin-labeled microtubules that were stabilized by GMPCPP were fixed on avidin-coated coverglasses. KIF19A diluted in PEM supplemented with 5 mM ATP and oxygen scavengers was introduced into the flow chamber. Time-lapse observation was performed using TIRF as described in the Microtubule Gliding Assay section.

SUPPLEMENTAL INFORMATION

Supplemental Information includes one figure, five movies, and Supplemental Experimental Procedures and can be found with this article online at http://dx.doi.org/10.1016/j.devcel.2012.10.016.

ACKNOWLEDGMENTS

The authors thank T. Yagi (University of Tokyo) for the *Chlamydomonas* axoneme experiments. The authors also thank H. Fukuda, T. Aizawa, T. Akamatsu, S. Hiromi, and others from the Hirokawa laboratory for discussions and technical assistance. N.H. planned and directed this research. K.N. prepared knockout mice. H.M. cloned KIF19A and prepared the antibody. Y.M. found the localization of KIF19A. D.W. purified the recombinant KIF19A. S.N. performed microscope experiments and biochemical analyses. S.N. and N.H. found the ciliary elongation and prepared the manuscript. This study was supported by Carl Zeiss, JEOL, and a Grant-in-Aid for Specially Promoted Research to N.H. from the Ministry of Education, Culture, Sports, Science and Technology of Japan.

Received: July 5, 2012
Revised: October 4, 2012
Accepted: October 15, 2012
Published online: November 15, 2012

REFERENCES

Aizawa, H., Sekine, Y., Takemura, R., Zhang, Z., Nangaku, M., and Hirokawa, N. (1992). Kinesin family in murine central nervous system. J. Cell Biol. *119*, 1287–1296.

Akella, J.S., Wloga, D., Kim, J., Starostina, N.G., Lyons-Abbott, S., Morrissette, N.S., Dougan, S.T., Kipreos, E.T., and Gaertig, J. (2010). MEC-17 is an alpha-tubulin acetyltransferase. Nature *467*, 218–222.

Anderson, R.G. (1974). Isolation of ciliated or unciliated basal bodies from the rabbit oviduct. J. Cell Biol. *60*, 393–404.

Berman, S.A., Wilson, N.F., Haas, N.A., and Lefebvre, P.A. (2003). A novel MAP kinase regulates flagellar length in Chlamydomonas. Curr. Biol. *13*, 1145–1149.

Binder, L.I., Dentler, W.L., and Rosenbaum, J.L. (1975). Assembly of chick brain tubulin onto flagellar microtubules from Chlamydomonas and sea urchin sperm. Proc. Natl. Acad. Sci. USA *72*, 1122–1126.

Blaineau, C., Tessier, M., Dubessay, P., Tasse, L., Crobu, L., Pagès, M., and Bastien, P. (2007). A novel microtubule-depolymerizing kinesin involved in length control of a eukaryotic flagellum. Curr. Biol. *17*, 778–782.

Carter, N., and Cross, R. (2001). An improved microscope for bead and surface-based motility assays. Methods Mol. Biol. *164*, 73–89.

Chan, K.Y., and Ersfeld, K. (2010). The role of the Kinesin-13 family protein TbKif13-2 in flagellar length control of Trypanosoma brucei. Mol. Biochem. Parasitol. *174*, 137–140.

Dawson, S.C., Sagolla, M.S., Mancuso, J.J., Woessner, D.J., House, S.A., Fritz-Laylin, L., and Cande, W.Z. (2007). Kinesin-13 regulates flagellar, interphase, and mitotic microtubule dynamics in Giardia intestinalis. Eukaryot. Cell *6*, 2354–2364.

Desai, A., and Mitchison, T.J. (1998). Preparation and characterization of caged fluorescein tubulin. Methods Enzymol. *298*, 125–132.

Desai, A., Verma, S., Mitchison, T.J., and Walczak, C.E. (1999). Kin I kinesins are microtubule-destabilizing enzymes. Cell *96*, 69–78.

Dishinger, J.F., Kee, H.L., Jenkins, P.M., Fan, S., Hurd, T.W., Hammond, J.W., Truong, Y.N., Margolis, B., Martens, J.R., and Verhey, K.J. (2010). Ciliary entry of the kinesin-2 motor KIF17 is regulated by importin-beta2 and RanGTP. Nat. Cell Biol. *12*, 703–710.

Gupta, M.L., Jr., Carvalho, P., Roof, D.M., and Pellman, D. (2006). Plus end-specific depolymerase activity of Kip3, a kinesin-8 protein, explains its role in positioning the yeast mitotic spindle. Nat. Cell Biol. *8*, 913–923.

Hertzer, K.M., Ems-McClung, S.C., Kline-Smith, S.L., Lipkin, T.G., Gilbert, S.P., and Walczak, C.E. (2006). Full-length dimeric MCAK is a more efficient microtubule depolymerase than minimal domain monomeric MCAK. Mol. Biol. Cell *17*, 700–710.

Hirokawa, N., Tanaka, Y., Okada, Y., and Takeda, S. (2006). Nodal flow and the generation of left-right asymmetry. Cell *125*, 33–45.

Hirokawa, N., Noda, Y., Tanaka, Y., and Niwa, S. (2009). Kinesin superfamily motor proteins and intracellular transport. Nat. Rev. Mol. Cell Biol. *10*, 682–696.

Homma, N., Takei, Y., Tanaka, Y., Nakata, T., Terada, S., Kikkawa, M., Noda, Y., and Hirokawa, N. (2003). Kinesin superfamily protein 2A (KIF2A) functions in suppression of collateral branch extension. Cell *114*, 229–239.

Howard, J., and Hyman, A.A. (2007). Microtubule polymerases and depolymerases. Curr. Opin. Cell Biol. *19*, 31–35.

Huang, K., Diener, D.R., and Rosenbaum, J.L. (2009). The ubiquitin conjugation system is involved in the disassembly of cilia and flagella. J. Cell Biol. *186*, 601–613.

Hubbert, C., Guardiola, A., Shao, R., Kawaguchi, Y., Ito, A., Nixon, A., Yoshida, M., Wang, X.F., and Yao, T.P. (2002). HDAC6 is a microtubule-associated deacetylase. Nature *417*, 455–458.

Hunter, A.W., Caplow, M., Coy, D.L., Hancock, W.O., Diez, S., Wordeman, L., and Howard, J. (2003). The kinesin-related protein MCAK is a microtubule depolymerase that forms an ATP-hydrolyzing complex at microtubule ends. Mol. Cell *11*, 445–457.

Ibañez-Tallon, I., Heintz, N., and Omran, H. (2003). To beat or not to beat: roles of cilia in development and disease. Hum. Mol. Genet. *12*(Spec No 1), R27–R35.

Ishikawa, H., and Marshall, W.F. (2011). Ciliogenesis: building the cell's antenna. Nat. Rev. Mol. Cell Biol. *12*, 222–234.

Kamiya, R. (2002). Functional diversity of axonemal dyneins as studied in Chlamydomonas mutants. Int. Rev. Cytol. *219*, 115–155.

Kanai, Y., Okada, Y., Tanaka, Y., Harada, A., Terada, S., and Hirokawa, N. (2000). KIF5C, a novel neuronal kinesin enriched in motor neurons. J. Neurosci. *20*, 6374–6384.

Kozminski, K.G., Beech, P.L., and Rosenbaum, J.L. (1995). The Chlamydomonas kinesin-like protein FLA10 is involved in motility associated with the flagellar membrane. J. Cell Biol. *131*, 1517–1527.

Lawrence, C.J., Dawe, R.K., Christie, K.R., Cleveland, D.W., Dawson, S.C., Endow, S.A., Goldstein, L.S., Goodson, H.V., Hirokawa, N., Howard, J., et al. (2004). A standardized kinesin nomenclature. J. Cell Biol. *167*, 19–22.

Lyons, R.A., Saridogan, E., and Djahanbakhch, O. (2006). The reproductive significance of human Fallopian tube cilia. Hum. Reprod. Update *12*, 363–372.

Mayr, M.I., Hümmer, S., Bormann, J., Grüner, T., Adio, S., Woehlke, G., and Mayer, T.U. (2007). The human kinesin Kif18A is a motile microtubule depolymerase essential for chromosome congression. Curr. Biol. *17*, 488–498.

Miki, H., Setou, M., Kaneshiro, K., and Hirokawa, N. (2001). All kinesin superfamily protein, KIF, genes in mouse and human. Proc. Natl. Acad. Sci. USA *98*, 7004–7011.

Mitchison, T., and Kirschner, M. (1984). Dynamic instability of microtubule growth. Nature *312*, 237–242.

Nakajima, K., Takei, Y., Tanaka, Y., Nakagawa, T., Nakata, T., Noda, Y., Setou, M., and Hirokawa, N. (2002). Molecular motor KIF1C is not essential for mouse survival and motor-dependent retrograde Golgi apparatus-to-endoplasmic reticulum transport. Mol. Cell. Biol. *22*, 866–873.

Noda, Y., Niwa, S., Homma, N., Fukuda, H., Imajo-Ohmi, S., and Hirokawa, N. (2012). Phosphatidylinositol 4-phosphate 5-kinase alpha (PIPKα) regulates neuronal microtubule depolymerase kinesin, KIF2A and suppresses elongation of axon branches. Proc. Natl. Acad. Sci. USA *109*, 1725–1730.

O'Hagan, R., Piasecki, B.P., Silva, M., Phirke, P., Nguyen, K.C., Hall, D.H., Swoboda, P., and Barr, M.M. (2011). The tubulin deglutamylase CCPP-1 regulates the function and stability of sensory cilia in C. elegans. Curr. Biol. *21*, 1685–1694.

Okada, Y., Yamazaki, H., Sekine-Aizawa, Y., and Hirokawa, N. (1995). The neuron-specific kinesin superfamily protein KIF1A is a unique monomeric motor for anterograde axonal transport of synaptic vesicle precursors. Cell *81*, 769–780.

Omori, Y., Chaya, T., Katoh, K., Kajimura, N., Sato, S., Muraoka, K., Ueno, S., Koyasu, T., Kondo, M., and Furukawa, T. (2010). Negative regulation of ciliary length by ciliary male germ cell-associated kinase (Mak) is required for retinal photoreceptor survival. Proc. Natl. Acad. Sci. USA *107*, 22671–22676.

Piao, T., Luo, M., Wang, L., Guo, Y., Li, D., Li, P., Snell, W.J., and Pan, J. (2009). A microtubule depolymerizing kinesin functions during both flagellar disassembly and flagellar assembly in Chlamydomonas. Proc. Natl. Acad. Sci. USA *106*, 4713–4718.

Rosenbaum, J.L., and Witman, G.B. (2002). Intraflagellar transport. Nat. Rev. Mol. Cell Biol. *3*, 813–825.

Satir, P., and Christensen, S.T. (2007). Overview of structure and function of mammalian cilia. Annu. Rev. Physiol. *69*, 377–400.

Scholey, J.M., Porter, M.E., Grissom, P.M., and McIntosh, J.R. (1985). Identification of kinesin in sea urchin eggs, and evidence for its localization in the mitotic spindle. Nature *318*, 483–486.

Sharma, N., Bryant, J., Wloga, D., Donaldson, R., Davis, R.C., Jerka-Dziadosz, M., and Gaertig, J. (2007). Katanin regulates dynamics of microtubules and biogenesis of motile cilia. J. Cell Biol. *178*, 1065–1079.

Shi, D., Komatsu, K., Uemura, T., and Fujimori, T. (2011). Analysis of ciliary beat frequency and ovum transport ability in the mouse oviduct. Genes Cells *16*, 282–290.

Stout, J.R., Yount, A.L., Powers, J.A., Leblanc, C., Ems-McClung, S.C., and Walczak, C.E. (2011). Kif18B interacts with EB1 and controls astral microtubule length during mitosis. Mol. Biol. Cell *22*, 3070–3080.

Su, X., Qiu, W., Gupta, M.L., Jr., Pereira-Leal, J.B., Reck-Peterson, S.L., and Pellman, D. (2011). Mechanisms underlying the dual-mode regulation of microtubule dynamics by Kip3/kinesin-8. Mol. Cell *43*, 751–763.

Tam, L.W., Wilson, N.F., and Lefebvre, P.A. (2007). A CDK-related kinase regulates the length and assembly of flagella in Chlamydomonas. J. Cell Biol. *176*, 819–829.

Tammachote, R., Hommerding, C.J., Sinders, R.M., Miller, C.A., Czarnecki, P.G., Leightner, A.C., Salisbury, J.L., Ward, C.J., Torres, V.E., Gattone, V.H., 2nd, and Harris, P.C. (2009). Ciliary and centrosomal defects associated with mutation and depletion of the Meckel syndrome genes MKS1 and MKS3. Hum. Mol. Genet. *18*, 3311–3323.

Vale, R.D., Reese, T.S., and Sheetz, M.P. (1985). Identification of a novel force-generating protein, kinesin, involved in microtubule-based motility. Cell *42*, 39–50.

Varga, V., Helenius, J., Tanaka, K., Hyman, A.A., Tanaka, T.U., and Howard, J. (2006). Yeast kinesin-8 depolymerizes microtubules in a length-dependent manner. Nat. Cell Biol. *8*, 957–962.

Varga, V., Leduc, C., Bormuth, V., Diez, S., and Howard, J. (2009). Kinesin-8 motors act cooperatively to mediate length-dependent microtubule depolymerization. Cell *138*, 1174–1183.

Wloga, D., Webster, D.M., Rogowski, K., Bré, M.H., Levilliers, N., Jerka-Dziadosz, M., Janke, C., Dougan, S.T., and Gaertig, J. (2009). TTLL3 Is a tubulin glycine ligase that regulates the assembly of cilia. Dev. Cell *16*, 867–876.

Yagi, T., Uematsu, K., Liu, Z., and Kamiya, R. (2009). Identification of dyneins that localize exclusively to the proximal portion of Chlamydomonas flagella. J. Cell Sci. *122*, 1306–1314.

Zhou, R., Niwa, S., Homma, N., Takei, Y., and Hirokawa, N. (2009). KIF26A is an unconventional kinesin and regulates GDNF-Ret signaling in enteric neuronal development. Cell *139*, 802–813.